

# Theoretical resolution of the $H^-$ resonance spectrum up to the $n=4$ threshold.

## I. States of $^1P^o$ , $^1D^o$ , and $^1F^o$ symmetries

Miroslaw Bylicki<sup>1,\*</sup> and Cleanthes A. Nicolaides<sup>2,†</sup><sup>1</sup>*Instytut Fizyki, Uniwersytet Mikołaja Kopernika, Grudziądzka 5, 87-100 Toruń, Poland*<sup>2</sup>*Physics Department, National Technical University, Athens, and Theoretical and Physical Chemistry Institute, National Hellenic Research Foundation, 48 Vas. Constantinou Avenue, 11635 Athens, Greece*

(Received 9 August 1999; published 12 April 2000)

We report on a theoretical approach to the calculation of wave functions, energies  $E$ , and widths  $\Gamma$  of high-lying resonances of  $H^-$ , with application to the identification of 76 states of  $^1P^o$ ,  $^1D^o$ , and  $^1F^o$  symmetries up to the  $n=4$  threshold, with widths down to about  $1 \times 10^{-8} - 1 \times 10^{-10}$  a.u., depending on symmetry and threshold. The overwhelming majority of these resonances have not been detected experimentally. Previous calculations by different methods allowed the identification of 35 of these states, with only very few cases having a level of accuracy comparable to the one of the present work. We suggest that the measurement of these resonances might become possible via two-step excitation mechanisms using ultrasensitive techniques capable of dealing with the problems of very small widths and preparation cross-sections. In this work, the  $^1D$  state at 10.872 eV above the  $H^- 1s^2 \ ^1S$  ground state, already prepared and measured by electron scattering as well as by two-photon absorption, is considered as the stepping stone for the possible probing of resonances of  $^1P^o$ ,  $^1D^o$ , and  $^1F^o$  symmetries via absorption of tunable radiation of high resolution. By classifying the results according to the Gailitis-Damburg model of *dipole resonances* (a product of a  $1/r^2$ -like potential) we find that there are unperturbed as well as perturbed series, in analogy with the Rydberg spectra of neutrals and positive ions (a product of a  $1/r$ -like potential). For the former, the agreement with the Gailitis-Damburg predictions as to the relationship of the extent of the outer orbital and of the energies and widths of states is excellent. The perturbed series result from interchannel coupling and the remaining electron correlation. One of the effects is the existence of overlapping resonances. For example, for two  $^1P^o$  states below the  $n=3$  threshold there is degeneracy on the energy axis ( $E_1 = -0.0555763612$  a.u. and  $E_2 = -0.0555763099$  a.u.) but the widths differ ( $\Gamma_1 = 1.14 \times 10^{-4}$  eV and  $\Gamma_2 = 5.45 \times 10^{-6}$  eV). We also comment on whether consideration of the relativistic Lamb shift splitting of the hydrogen thresholds is sufficient for deciding the truncation of the resonance series. Our calculations were carried out by implementing previously published theories, whereby the resonance  $E$ 's and  $\Gamma$ 's are determined from properly selected complex eigenvalues of non-Hermitian Hamiltonian matrices constructed in terms of physically relevant square integrable real and complex function spaces representing the localized and asymptotic parts of the resonance eigenfunctions. For the  $H^-$  series of resonances, the physical relevance of the real functions implies the systematic construction of basis sets with average  $\langle r \rangle$  extending to thousands of atomic units, in order to account for the extreme diffuseness of the outer orbital as each threshold is approached. The complex one-electron basis sets are Slater-type orbitals of a complex coordinate  $re^{-i\theta}$ . Their inclusion into the overall calculation and their optimization via the variation of nonlinear parameters (including  $\theta$ ) accounts for the contribution of the asymptotic part of the resonance, and for the energy width and shift beyond the real energy  $E_o$  of the localized part.

PACS number(s): 31.50.+w, 32.80.Gc

### I. INTRODUCTION

The objective of the research reported here and in the accompanying paper [1], as well as in a recent letter [2], was to compute and analyze highly accurate resonance wave functions of the hydrogen negative ion  $H^-$ , and to completely resolve the resonance spectrum of  $H^-$  in the energy range up to the  $n=4$  threshold. (In Ref. [2], the calculation of states of  $^1P^e$  symmetry went up to the  $n=5$  threshold). By resolution, we mean the accurate identification of all the physically relevant complex poles of the resolvent  $R(z) \equiv (z - H)^{-1}$ , where  $z$  is a complex variable and  $H$  is the total Hamiltonian of the system. These poles are associated with nonstationary (resonance) states  $|\kappa\rangle$ , whose energy is com-

plex;  $z_\kappa = E_\kappa - (i/2)\Gamma_\kappa$ , where  $E_\kappa$  is the total energy and  $\Gamma_\kappa$  is the total width.

Nonstationary states in the continuum of atomic negative ions (ANI's) or of any other atomic or molecular system are represented by electronic structures signifying multiple excitation from, or electron attachment to, or creation of a hole in a subshell of a particular configuration. A research program since 1972 [3], whereby the computation and analysis of the wave functions and properties of these states is done by considering them in a unified manner as *decaying states* (see Refs. [3–12], and references therein) breaks down the overall calculation into two steps, regardless of the number of electrons, of electronic structure, and of level of excitation.

The first step emphasizes the state-specific analysis and application of advanced many-electron methods for the calculation of electronic structures representing the localized part of resonances,  $\psi_o^k$ . These structures may be characterized in zero order by one configuration or by a superposition

\*Electronic address: mirekb@phys.uni.torun.pl

†Electronic address: can@eie.gr

of a few configurations with outer or inner subshell holes, or with both, or may represent shape resonances associated with ground or excited configurations. In this context, it has been shown that state-specific Hartree-Fock (HF) or multiconfigurational HF (MCHF) equations can be solved in a meaningful way analytically or numerically, even for triply excited resonances of ANI's (e.g.,  $\text{He}^- 2s^2 2p^2 P^o, 2s 2p^2 D$ ). The HF or MCHF solutions represent optimal square-integrable wave functions with energies inside the continuous spectrum, and their validity is justified by following the convergence of the total energy to a local minimum based on localization criteria such as occupancy, extent, and nodal structure of the radials, and the satisfaction of the virial theorem. Such zero-order representations of nonstationary states allow the extraction of physically significant characteristics and an understanding of the extent to which *exchange* and *near-degeneracy* interactions, or *part of the continuum* contribute to the stability of the resonance. The remaining electron correlation which contributes to localization is added variationally. Both at zero order and all-order levels of calculation of  $\psi_o$ , by construction, and by orthogonalization (when necessary), the function space of the open channels leading to decay is excluded.

On the other hand, there are electronic structures of ANI resonances such as the ones treated in this work, where it is necessary to calculate  $\psi_o^k$  which are extremely diffuse, reaching to about, say, 5000 a.u. Therefore, different techniques, numerically very accurate, have to be applied. As we discuss in Secs. V and VI, given the wave-function features of the  $\text{H}^-$  resonances associated with each threshold, this problem has been solved here by using basis sets covering a large range with a systematically controlled position distribution, thereby allowing a "group of states" specific representation of  $\psi_o^k$ .

The second step addresses the issue of the incorporation of the effects of the multichannel (in general) continuum and of the final determination of the complex eigenvalue, without or with reoptimization of the components of  $\psi_o$ . The functions representing the asymptotic part of the resonance can be either numerical or suitably optimized analytic basis sets coupled to the appropriate term of the bound core. If real coordinates are employed, the procedures are based on multichannel reaction matrix theory [5,12]. If a basis set of complex coordinates is employed, as in the present work, the procedure involves construction and diagonalization of non-Hermitian matrices, from which the search for the eigenvalue  $z_\kappa$  is guided by conditions satisfied on resonance and by the fact that the overlap of the trial function with  $\psi_o^k$  must stay maximum (see Refs. [4,7–10], and references therein).

Calculations within the framework referred to above, with real or complex coordinates for the asymptotic components, have dealt with the calculation of positions and total and partial widths of a variety of states, ranging from doubly and triply excited ANI resonances, (e.g.,  $\text{He}^- 1s 2s 2p^2 P^o, 1s 2p^2 4P, 1s n l^2 4P, 2s, n=2,3, \dots, 6, 2s 2p^2 4P, 2P, 2D$  etc.), to inner hole Auger states (e.g.,  $\text{Be}^+ 1s 2s^2 2S, \text{Ne}^+ 1s 2s^2 2p^6 2S$ ). These calculations were done by first specifying the particular electronic configurations, regardless of their energy position. In this work we ask a different ques-

tion, demanding a much heavier load of computations: If we first specify a particular energy region in the continuous spectrum of a particular system, how can we uncover *all* the resonance states of a given symmetry in this region and produce their  $E_\kappa$  and  $\Gamma_\kappa$  reliably? The fact that  $\text{H}^-$  has only two electrons makes this question answerable to very high accuracy. At the same time, we stress that the theory is applicable to larger atoms as well, since the calculation of electronic structures corresponding to the various  $\psi_o^k$  of  $N$ -electron atoms and ions can be done efficiently with currently available computer power.

The case of  $\text{H}^-$  is the simplest ANI from the point of view of the number of electrons and of spin and angular momentum couplings. However, the quest for the identification, theoretically or experimentally, of all the resonances of a particular symmetry within a given energy range is plagued by the predictions of Gailitis and Damburg (GD), who introduced the model of  $\text{H}^-$  "dipole resonances" [13] (see also Refs. [14–17]). Accordingly, for a specific combination of symmetry and thresholds, the number of resonances below each threshold is infinite, with their spatial extent growing exponentially and their widths decreasing exponentially, where the exponents are given by the theory of the model. It follows that the burden for *ab initio* theory is to achieve the identification of resonances whose widths are expected to decrease rapidly to extremely small values as threshold is approached (say  $\sim 10^{-10}$  eV). The question that then arises is where to stop the calculation of  $E_\kappa$  and  $\Gamma_\kappa$  as  $|\kappa\rangle$  approach the corresponding threshold [18], so as to have, on the one hand, a definitive picture of the properties of  $\text{H}^-$  resonances and, on the other hand, to avoid the expense of computational effort in seeking insignificant information. Given the fact that the herein suggested (Sec. II) dye-laser experiments based on two-step excitation mechanisms should produce, in principle, resolution of the order of  $0.02\text{--}0.002\text{ cm}^{-1}$  ( $10^{-7}\text{--}10^{-8}$  a.u.), we thought it reasonable to adopt widths as low as  $1 \times 10^{-8}\text{--}1 \times 10^{-10}$  a.u., as a cutoff criterion for the search of  $\text{H}^-$  resonances, depending on the hydrogen threshold. This is an extremely small decay width for a many-electron resonance state and the goal of computing such a property accurately as the excitation energy increases considerably raises the demands on theory as regards computational completeness, efficiency, and numerical precision.

In the following sections we discuss the choice of the states studied and the previous results for them, the theoretical background, and the framework for the calculation of resonances of  $N$ -electron atoms and ions, the present implementation of which is particular to  $\text{H}^-$ , and our results. The total number of resonances of  $1P^o, 1D^o$ , and  $1F^o$  symmetry that were computed, and which constitute the  $\text{H}^-$  resonance spectrum up to the  $n=4$  threshold subject to the cutoff criterion, is 76. Of these, 41 are predicted here for the first time, to our knowledge, while for the ones already calculated by a number of researchers since the 1960s, the present level of accuracy is higher, with the exception of recent results for the  $1P^o$  resonances below the  $n=2$  threshold (see Sec. III and Table I), which are also characterized by a high degree of numerical accuracy. In addition to values for  $E_\kappa$  and  $\Gamma_\kappa$ , we calculate wave-function characteristics along the series,

TABLE I. Energies and widths of  $H^- 1P^o$  Feshbach resonances below the  $n=2$  threshold.

State	CI close coupling		CCR		Algebraic close coupling		CESE	
	Venuti and Decleva [42]		Lindroth <i>et al.</i> [43]		Gien [45]		This work	
	$-E$ (a.u.)	$\Gamma$ (a.u.)	$-E$ (a.u.)	$\Gamma$ (a.u.)	$-E$ (a.u.)	$\Gamma$ (a.u.)	$-E$ (a.u.)	$\Gamma$ (a.u.)
(1)	0.126049581	1.3669[6]	0.12604985975	1.37[6]	0.12604518	1.386[6]	0.126049837	1.3618[6]
(2)	0.125035391	7.2313[8]	0.125035052	7.4[8]	0.12503492	7.53[8]	0.1250350503	7.28[8]
(3)			0.1250012	2.2[9]	0.1250011892	2.6655[9]	0.12500119344	2.64[9]
(4)					0.125000039758	9.615[11]	0.1250000408	2[11]

such as the breakdown into components based on ( $ll'$ ) configurations, and the systematics of the average radius of the outer electron. All these data are used to establish the existence of unperturbed and perturbed series of  $H^-$  resonances with respect to the predictions of the GD model of dipole resonances.

## II. PRESENT CHOICE OF OBSERVABLE $H^-$ RESONANCES OTHER THAN THE PREVIOUSLY MEASURED LOW-LYING ONES

The nonrelativistic spectrum of each ANI is characterized by very few bound states and many resonances, corresponding to multiply excited configurations. As regards the bound excited states, experimental information is rather scarce, and it is mainly theory and computation that have provided knowledge of their existence and properties (See e.g., Ref. [19], and references therein). As regards the resonances, their preparation is in principle easier, due to the availability of more entrance channels. Nevertheless, the fact remains that the available spectroscopic data on resonances are still very few, while the measurement of the position,  $E$  and the width  $\Gamma$  of even a single resonance often constitutes a serious challenge. This is due to a superposition of limiting factors such as the general lack of easily prepared and controlled suitable initial states, the restrictions imposed by selection rules of energy difference and symmetry, and the requirements of high resolution when the resonances are narrow and/or the excitation cross section is very small. For example, consider  $H^-$ , the ANI of interest here. Even if one assumes the availability of a beam of  $1s^2 1S$  ground state ions and of tunable radiation in the range 0–15 eV with perfect resolution, one-photon absorption excites doubly excited states (DES's) of only  $1P^o$  symmetry in  $LS$  coupling, leaving out many other singlet and all triplet symmetries. (For one-photon absorption measurements of  $H^-$  DES's, see Refs. [20,21], and references therein. For the excitation of the lowest  $1D$  resonance at  $10.872 \pm 0.002$  eV above the  $H^-$  ground state via two-photon absorption, see Ref. [22]) [23].

The above limitations on observation and measurement can be rectified to some extent in three ways. The first is to perform electron-atom collision experiments, from which additional information, especially for the low-lying states below each threshold, can be obtained (see, e.g., Refs. [24–29] and references therein). This approach is limited by requirements of very high resolution which is necessary for very narrow resonances, as are the ones in  $H^-$  except the lowest-lying ones. The second is to be able to follow the decay

dynamics from higher-lying states excited in collisions, as, e.g., it is done with beam-foil spectroscopy. For example, in this way it became possible to observe, via its transition to the lower-lying  $He^- 1s2p^2 4P$  shape resonance, the triply excited  $2p^3 4S^o$  bound state of  $He^-$  [30]. However, the population and measurement of  $E$  and  $\Gamma$  of each resonance from decays of higher-lying states is not practically feasible, even via ultrasensitive techniques for fluorescence detection.

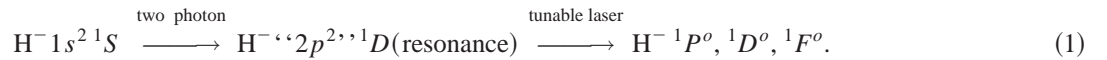
The third way is what we propose here as being the most promising one, if fully developed in the future, for measuring resonances which are high lying and have narrow widths and very small absorption oscillator strengths for a one-photon transition from a lower resonance. This is based on the possibility of using a two-step mechanism, rather than a direct excitation. Accordingly, the first step excites via one or more photons (high resolution but symmetry restricted) a resonance which serves as a stepping stone for the synchronized second excitation by a high-resolution tunable laser source. (Say a 20-Hz nanosecond R6G dye laser with resolution of about  $0.02 \text{ cm}^{-1}$ ).

An alternative to using a photon pulse as the first probe is to use an electron pulse. In this case, resolution is much lower (see below), but more symmetries are in principle reachable. For example, such a two-step excitation mechanism has been proposed for the creation of  $H^-$  triplets and, specifically, of the  $H^- 2p^2 3P$  bound state which is used for the subsequent study of the variation of widths of two or more triplet DES's coupled by external ac or dc fields [8].

Here we note that in the case of a one-photon resonance-resonance transition with a broad-band excitation of the initial state, a recent theory taking into account the contribution of the free-free dipole transition moment has produced the form of the absorption profile, with a quantitative application to the  $He 2s2p^1 P^o \rightarrow 1D$  transition [31]. When electron excitation is used as the first step, restrictions of resolution allow the detection of only the lowest lying  $H^-$  Feshbach resonances or of possible *shape* resonances associated with each threshold [24–29]. If one assumes that a certain such state is created, further excitation by narrow width tunable laser will be useless in detecting narrow higher-lying states because of the much larger width of the initial state. A way out is to utilize accurate theoretical data on  $E$  and  $\Gamma$ , such as the ones presented in this paper, in the following way: Knowing the positions of the states which are collectively excited by the electron wave packet and knowing their widths, the shot of the laser can be synchronized for further excitation after different durations corresponding approxi-

mately to lifetimes of states to be excited. (Say 1, 5, 10, etc. ns). By this time the broader lower states, with lifetimes say of the order of 100–900 fs, will have decayed and the second excitation wave packet will be narrow enough to resolve a number of higher-lying states via ultrasensitive fluorescence or field ionization techniques. Such measurements are probably possible if one starts with a  $H^-$  beam of about  $10^{12}$  atoms (say from the photolysis of HCl by a polarized 193-nm excimer laser pulse) and the  $e+H$  cross section for the formation of the initial  $H^-$  DES is of order of  $10 \text{ \AA}^2$  or larger.

The above arguments about the utility of a two-step excitation mechanism can be tested by taking advantage of the fact that the lowest  $^1D$  resonance has been prepared and measured under controlled conditions via two-photon absorption [22]. Although this state has also been measured in  $e-H$  collisions [32,28], it is the precision of laser excitation that permits the immediate possibility of a reliable execution of high resolution measurements of higher DES's using a second, tunable, laser. Thus the choice of the two-step mechanism in this case is



Suppose we consider the energy region up to the  $H$   $n=4$  threshold, which is 2.631 eV above the experimental position of the  $^1D$  state [23]. We then ask the question: *How many and which resonances of each symmetry are there whose  $E$  and  $\Gamma$  can be observed by measurements with resolution of, say,  $0.02\text{--}0.002 \text{ cm}^{-1}$  ( $\sim 10^{-7}\text{--}10^{-8} \text{ a.u.}$ )?* As already stated in Sec. I, given this energy region the cutoff lower limits for the widths which were searched for in our computations were in fact set at about  $1 \times 10^{-8}\text{--}1 \times 10^{-10} \text{ a.u.}$  The limit of the  $n=4$  threshold was chosen as providing a reasonable energy range for the testing of advanced theory of resonances without an exorbitant expense of time for computation. In addition, this range is also convenient for high-resolution measurements via tunable photon absorption using dye lasers. Of course, the limit of observability of the high-lying and very diffuse resonances will also be determined by the size of the oscillator strengths and the degree of sensitivity of the technique of measuring absorption coefficients.

### III. PREVIOUS RESULTS ON THE IDENTIFICATION OF $H^- {}^1P^o$ , ${}^1D^o$ , AND ${}^1F^o$ RESONANCES UP TO THE $n=4$ THRESHOLD

The resonance spectrum of  $H^-$  is the result of interactions of only three particles. Therefore, the relevant theory does not have to account for the complications characterizing arbitrary polyelectronic atomic states. This fact has facilitated the implementation of various *ab initio* methods and the model of dipole resonances since the early 1960s, when the first numbers on a few resonances were produced. Nevertheless, a reliable quantitative answer to the question posed in Sec. II has been lacking. (See the reviews by Schulz [25], Risley *et al.* [26], Williams [27,29], and Buckman and Clark [33] on ANI resonances, the papers cited here, and their references.) The basic reason for this fact is the requirement of generality of the theoretical method and of very high numerical accuracy that the computation must achieve. Such a calculation must account for the details of dynamical screening and polarization, configuration interaction, and interchannel coupling to all orders, and must be economical enough to be

carried out on a very fine energy (real or complex) mesh. Otherwise, its results on the resolution of the resonance spectrum are bound to be incomplete. (For example, only the few “easy” cases may be identified.)

For example, let us consider the most extensively studied symmetry,  ${}^1P^o$ , and the question of the number and properties of its resonances below the  $n=2$  threshold. In this paper we report on the existence and properties of four such non-relativistic resonances, two of them below the relativistic  $2p_{1/2}$  threshold (Sec. VI). However, large-scale calculations following the  $R$  matrix [34–36] or the complex coordinate rotation (CCR) [37,38] methods, have identified only one such  ${}^1P^o$  resonance. In fact, the positions of the first two were predicted by O'Malley and Geltman in 1965 [39], via their pioneering variational calculations on the roots of the explicitly constructed Feshbach  $QHQ$  Hamiltonian. They reported  $E({}^1P^o(1))=10.927 \text{ eV}$  and  $E({}^1P^o(2))=10.953 \text{ eV}$  above the  $H^- 1s^2 {}^2S$  ground state. The experimental verification of the second  ${}^1P^o$  resonance was first achieved in a recent photoabsorption experiment by Andersen *et al.* [21], where the energy was measured at 10.9519 eV but the resolution was not high enough to deduce the width. The first prediction of this width was made in 1971 by Seiler, Oberoi, and Callaway [40] who implemented the Harris-Nesbet algebraic close-coupling method. Using four coupled channels, they found  $E=10.958 \text{ eV}$  and  $\Gamma=2.06 \times 10^{-7} \text{ eV}$ . Much later, a more accurate theoretical prediction (especially for the width), which preceded the photoabsorption experiment by a few years, was given by Cortés and Martín [41], who implemented Feshbach's scattering formalism with  $\mathcal{L}^2$  basis sets, to carry out calculations of the photoabsorption cross section. Their values are  $E=10.9522 \text{ eV}$  and  $\Gamma=1.7 \times 10^{-6} \text{ eV}$ . A similar basis set expansion calculation by Venuti and Decleva [42] also produced accurate results for the first two  ${}^1P^o$  resonances. (See Table I for a collection of results of  ${}^1P^o$  resonances below the  $n=2$  threshold.)

A prediction for the position of a third  ${}^1P^o$  resonance (10.9531 eV above  $H^- 1s^2$ , if we use 1 a.u. = 27.19658 eV) was given in 1965 by Temkin and Walker

TABLE II. Energies and widths of  $H^{-1}P^o$  Feshbach resonances below the  $n=3$  threshold.

State	R matrix		CCR		CI close coupling		CESE			
	Pathak <i>et al.</i> [34] −E (a.u.)	Γ (a.u.)	Ho [87] −E (a.u.)	Γ (a.u.)	Lindroth [88] −E (a.u.)	Γ (a.u.)	Venuti and Decleva [42] −E (a.u.)	Γ (a.u.)	This work −E (a.u.)	Γ (a.u.)
(1)	0.062713	1.255[3]	0.06271675	1.1915[3]	0.06273	1.199[3]	0.06271651	1.19126[3]	0.06271692	1.19006[3]
(2)	0.0585715	9.0[6]	0.0585718	8.99[6]	0.05857	8.8[6]	0.0585697	8.968[6]	0.0585718096	8.9874[6]
(3)	0.056145		0.0561167	2.1[6]	0.05612	2.2[6]	0.05611661	2.136[6]	0.056116399	2.2578[6]
(4)	0.055903	6.65[5]	0.055907	7.0[5]	0.05590	7.096[5]	0.0559045	7.061[5]	0.05590626	7.0948[5]
(5)					0.05566	4[7]	0.05566923	4.611[7]	0.0556630559	3.9548[7]
(6)					0.05558	4[6]	0.05557517	4.067[6]	0.0555763612	4.1854[6]
(7)							0.055577623	1.188[8]	0.0555763099	2.0030[7]
(8)							0.055559828	1.760[8]	0.055559575918	1.5172[8]
(9)							0.055556725	2.444[7]	0.05555679529	2.5698[7]
(10)									0.055556333474	2.901[9]
(11)									0.05555570632	5.88[10]
(12)									0.05555562951	1.5280[7]
(13)									0.055555583	1.1[8]

[14] without an *ab initio* calculation. Instead, they applied the Gailitis-Damburg formula [13] [see Eq. (18) below] normalized to the lowest root of the  $QHQ$  results of Ref. [39]. Higher energies of  $^1P^o$  resonances were not given since, by following the argument first given by Gailitis and Damburg, they considered that the series of resonances must stop below the relativistic  $2p_{1/2}$  level. More than 30 years later [43,44], the third  $^1P^o$  resonance was calculated *ab initio*, including the coupling to the continuum. By adding relativistic corrections, Lindroth *et al.* [43] found it to lie below the  $2p_{1/2}$  threshold. Again, the claim was made that this is the last one in this energy range, due to the relativistic splitting of the  $n=2$  threshold. We return to this issue in Sec. IV. Finally, in a very recent paper, Gien [45] presented very accurate non-relativistic results to many decimal digits for four  $^1P^o$  resonances below the  $n=2$  threshold, obtained by the algebraic close-coupling method.

For the region between  $n=2$  and 4 [46], there are experimental observations of a couple of  $^1P^o$  resonances [20,29] as well as a few theoretical results mainly on low-lying  $^1P^o$  resonances (see Tables II and III). Thus far, the largest number of  $^1P^o$  states identified below the  $n=3$  threshold in that achieved by the calculations of Venuti and Decleva [42] (nine states), while for  $^1P^o$  states below the  $n=4$  threshold, Pathak *et al.* [34] identified nine states. No shape resonances above the  $n=3$  and 4 thresholds have been predicted. One of the important findings of the measurements [20] is that the preferred decay channel is the one nearest, in agreement with earlier theoretical predictions and explanations [7,47].

As regards the  $^1D^o$  and  $^1F^o$  symmetries, the existing theoretical predictions of  $E$  and  $\Gamma$  are as follows: The implementation and application by Callaway and co-workers [48–50] of the algebraic close-coupling approach led to the prediction of one  $^1F^o$  below  $n=3$  [48,49] and one  $^1F^o$  and one  $^1D^o$  below  $n=4$  [50]. Lipsky *et al.* [51] predicted two  $^1D^o$  states and two  $^1F^o$  states below the  $n=3$  threshold, obtained from the roots of the truncated diagonalization method with hydrogenic functions. No widths are given [52].

By applying the CCR technique [53–55], Ho, Bhatia, and Callaway [56–58] have predicted one  $^1D^o$  and  $^1F^o$  resonances below the  $n=3$  threshold [57,58], one  $^1F^o$  shape resonance above  $E_{n=3}$  [57], and one  $^1D^o$  and two  $^1F^o$  Feshbach resonances below  $E_{n=4}$  [56]. Finally, two sets of  $R$ -matrix calculations produced one  $^1D^o$  resonance and one  $^1F^o$  resonance below  $E_{n=3}$  [34,35], and four  $^1D^o$  resonances and four  $^1F^o$  resonances below  $E_{n=4}$  [34]. A collection of results for  $^1D^o$  and  $^1F^o$  resonances is given in Tables IV and V.

#### IV. THEORY: FRAMEWORK OF THE PRESENT CALCULATIONS

In general, there are two ways to define and identify ( $E$  and  $\Gamma$ ) resonance states of a particular symmetry in the energy representation. One is to follow the changes of the scattering phase shift (or of the related  $S$  matrix) as a function of real energy and to deduce  $E$  and  $\Gamma$  from the conditions that, according to scattering theory, are satisfied on resonance. The other is to look for the solution of an appropriate relation producing directly a complex energy,  $z_o = E - (i/2)\Gamma$ . Anyway, the important issue as regards the physics of real  $N$ -electron systems is the possibility of computing accurately  $E$  and  $\Gamma$  either for single states or for series of resonances expected to exist in a particular energy region. In some relatively simple cases, such an accurate computation has proven, over a few decades of research on resonance states, feasible by a number of methods. However, in the general case of arbitrary structures and/or of arbitrary energy range, the requirements on theory and computation are stringent. In recognition of this challenging difficulty, a number of publications since 1972 (see, e.g., Refs. [3,5–12,59–62]) have presented a theoretical framework for the identification and calculation of arbitrary excited states in the continuous spectrum which emphasizes the significance of developing formalism and methods that use physically appropriate and computationally manageable function spaces. These one- and

TABLE III. Energies and widths of  $H^{-1}P^o$  Feshbach resonances below the  $n=4$  threshold.

State	R matrix		CCR				CESE	
	Pathak <i>et al.</i> [34]		Ho [87]		Lindroth [88]		This work	
	$-E$ (a.u.)	$\Gamma$ (a.u.)	$-E$ (a.u.)	$\Gamma$ (a.u.)	$-E$ (a.u.)	$\Gamma$ (a.u.)	$-E$ (a.u.)	$\Gamma$ (a.u.)
(1)	0.0371305	1.245[3]	0.03717945	1.0336[3]	0.03718	1.03[3]	0.0371794	1.034328[3]
(2)	0.034289	1.80[5]	0.03429405	1.83[5]	0.03430	1.84[5]	0.03429397	1.8328[5]
(3)	0.032324	2.25[4]	0.0323525	2.44[4]	0.03235	2.4[4]	0.032350629	2.4152[4]
(4)	0.032192	8.0[6]	0.0321985	7.7[6]	0.03220	7.7[6]	0.032198287	7.9216[6]
(5)	0.0316025		0.031613	5.95[6]	0.03161	6.6[6]	0.031613080	5.958[6]
(6)	0.0315535	4.65[5]	0.031562	3.15[6]	0.03156	2.2[6]	0.03155516	2.716[6]
(7)	0.0313515		0.0314975	6.47[5]	0.03150	6.3[5]	0.03149750	7.550[5]
(8)							0.031349759	8.718[7]
(9)	0.0313115		0.031315	1.2[4]			0.03132298	1.13866[4]
(10)	0.0313045				0.03131	1.5[5]	0.031304250	1.1694[5]
(11)							0.031282674	2.86[7]
(12)							0.0312645831	2.614[7]
(13)							0.0312627480	2.5110[6]
(14)							0.031260682	9.4[8]
(15)							0.0312535114	3.24[8]
(16)							0.03125293164	5.788[7]
(17)							0.0312511519	1.054[8]
(18)							0.03125067253	1.338[7]
(19)							0.03125053534	9.50[9]
(20)							0.0312503765	3.80[9]
(21)							0.0312501542	3.10[8]
(22)							0.031250120	3.4[9]
(23)							0.0312500159	1.34[9]
(24)							0.0312500172	1.8[8]

$N$ -electron function spaces consist of parts which are optimized separately and which represent, on the one hand, the short- and long-range self-consistent correlations contributing to localization,  $(\psi_o, E_o)$ , and, on the other hand, the coupled open channels whose mixing with  $\psi_o$  produces the final characteristics of the eigenfunction and of the intrinsic properties of the resonance state.

Given this framework and based on our previous experience with accurate calculations of doubly and triply excited resonances [9,63,64], we considered that a comprehensive cover of the  $^1P^o$ ,  $^1D^o$ , and  $^1F^o$   $H^{-}$  resonance spectra up to

the  $n=4$  threshold would be a feasible project. The foundations of our approach are briefly presented below.

### A. Complex eigenvalue Schrödinger equation

In the energy region where the resonance structure appears, the exact scattering state  $\psi(E)$  is a superposition of bound and energy-normalized scattering components. Appropriate relations among diagonal and off-diagonal matrix elements led to formulas for the energy-dependent phase shift, and for the position and width of the resonance [65,66].

TABLE IV. Energies and widths of  $H^{-1}D^o$  and  $^1F^o$  Feshbach resonances below the  $n=3$  threshold.

State	R matrix				CCR				CESE	
	Pathak <i>et al.</i> [34]		Odgers <i>et al.</i> [35]		Bhatia and Ho [58]		Ho [57]		This work	
	$-E$ (a.u.)	$\Gamma$ (a.u.)	$-E$ (a.u.)	$\Gamma$ (a.u.)	$-E$ (a.u.)	$\Gamma$ (a.u.)	$-E$ (a.u.)	$\Gamma$ (a.u.)	$-E$ (a.u.)	$\Gamma$ (a.u.)
$^1D^o(1)$	0.0594095	2.755[4]	0.05943	2.645[4]	0.059431007	2.49901[4]			0.059430923	2.4991[4]
(2)									0.0555997787	2.6768[6]
(3)									0.055556101835	3.3034[8]
$^1F^o(1)$	0.056558	5.5[6]	0.056875				0.0565588	5.02[6]	0.0565587519	5.0068[6]
(2)									0.05565771162	5.5402[7]
(3)									0.05556643170	5.972[8]
(4)									0.055556720982	6.408[9]
(5)									0.0555556809	6.8[10]

TABLE V. Energies and widths of  $H^{-1}D^o$  and  ${}^1F^o$  Feshbach resonances below the  $n=4$  threshold.

State	R-matrix Pathak <i>et al.</i> [34]		Variational close coupling Callaway [50]		CCR Ho and Callaway [56]		CESE This work	
	$-E$ (a.u.)	$\Gamma$ (a.u.)	$-E$ (a.u.)	$\Gamma$ (a.u.)	$-E$ (a.u.)	$\Gamma$ (a.u.)	$-E$ (a.u.)	$\Gamma$ (a.u.)
${}^1D^o(1)$	0.036498	1.175[3]	0.03635	1.25[3]	0.03652	1.2[3]	0.0365292	1.2286[3]
(2)	0.032067	2.16[4]					0.03209299	2.50202[4]
(3)	0.031709	7.0[6]					0.03171549133	7.42094[6]
(4)	0.0314025	4.55[5]					0.031416853	5.4614[5]
(5)							0.0312835667	1.12238[5]
(6)							0.03127688546	4.9388[7]
(7)							0.0312567786	2.276[6]
(8)							0.03125144201	2.6238[8]
(9)							0.03125137195	4.6184[7]
(10)							0.0312502777	9.378[8]
(11)							0.03125007408	2.10[9]
${}^1F^o(1)$	0.035098	6.55[4]	0.03515	6.5[4]	0.035125	6.5[4]	0.03511423	6.550[4]
(2)	0.0334555	1.80[5]					0.033461482	2.042[5]
(3)	0.031846	6.5[6]					0.03184856	7.578[6]
(4)	0.031661	4.85[5]					0.03170402	7.946[5]
(5)					0.03147	5[4]	0.0314357	3.880[4]
(6)							0.031418432	2.052[6]
(7)							0.031317286	1.4470[5]
(8)							0.031297999	5.820[7]
(9)							0.0312746	2.06[5]
(10)							0.0312637636	1.874[7]
(11)							0.031260405	2.424[6]
(12)							0.0312539447	4.90[8]
(13)							0.0312515877	3.660[7]
(14)							0.03125113086	1.376[8]
(15)							0.0312503239	4.72[9]
(16)							0.0312502433	5.562[8]
(17)							0.031250024	2.2[8]

The resonance state can be identified with a nonstationary state which is initially ( $t=0$ ) localized ( $\psi_o$ ), and which is decaying into the adjacent continuous spectrum spanned by the background scattering wave functions [3,11]. The physics of this picture implies that, on resonance, the asymptotic form of the scattering state,  $\psi(E)$ , represents the outgoing wave only. By combining the above, it has been shown [67,68] how a complex eigenvalue Schrödinger equation (CESE) describing resonances (*shape* or Feshbach) in short range, Coulomb and linear (dc-ac Stark effect) potentials, emerges simply but rigorously.

Specifically, following Fano [65], the scattering state function  $\psi(r;E)$  expressing the superposition of  $\psi_o(r)$  with the scattering functions,  $\mathcal{U}(r;E)$  of the continuous spectrum into which it is embedded, can be written as

$$\psi(r;E) = a(E) \left[ \psi_o(r) + P \int dE' \frac{V_{oE'}}{E-E'} \mathcal{U}(r;E') + \lambda(E) V_{oE} \mathcal{U}(r;E) \right], \quad (2)$$

which is valid for all values of the reaction coordinate  $r$  and satisfies the stationary state Schrödinger equation

$$(H-E)\psi(r;E) = 0 \quad (3)$$

for any real value of  $E$  in the continuous spectrum. In general, the matrix element  $V_{oE}$  mixing  $\psi_o(r)$  with  $\mathcal{U}(r;E)$  is given by

$$V_{oE} = \langle \mathcal{U}(r;E) | H - E_o | \psi_o(r) \rangle, \quad (4)$$

with

$$E_o = \langle \psi_o | H | \psi_o \rangle \text{ real} \quad (5)$$

and

$$E = E_o + P \int dE' \frac{|V_{oE'}|^2}{E-E'} + \lambda(E) |V_{oE}|^2. \quad (6)$$

Equations (2) and (6) constitute the definition of the function  $\lambda(E)$ , whose value is fixed by the asymptotic boundary conditions of the problem as follows: According to the physics of the decaying state, one must look at the asymptotic behavior of  $\Psi(r;E)$  which is obeyed under resonance conditions (i.e., under conditions of outgoing wave only). In doing so,  $\mathcal{U}(r;E)$  are represented by their asymptotic analytic

forms corresponding to a short-range potential (Bessel function), a Coulomb potential (Coulomb function), or to a linear potential (Airy function). By inserting these forms into Eq. (2) and by setting the ingoing wave part equal to zero, the value of  $\lambda(E)$  on resonance is found to be

$$\lambda(E) = -i\pi, \quad (7)$$

so that the energy in Eq. (6) becomes complex,

$$E \rightarrow z_o = E_o + P \int dE' \frac{|V_{oE'}|^2}{E - E'} - i\pi |V_{oE}|^2 = E_o + \Delta - \frac{i}{2}\Gamma, \quad (8)$$

where to lowest order and to a very good approximation  $\Delta(E) \approx \Delta(E_o)$  and  $\Gamma(E) \approx \Gamma(E_o)$ . On resonance, then, Eq. (3) becomes a CESE,

$$(H - z_o)\psi^{res}(r; z_o) = 0, \quad (9)$$

where the asymptotic boundary condition for  $\psi^{res}(r; z_o)$  is [67,68]

$$\psi^{res}(r; z_o) \sim b(z_o)e^{iNr}. \quad (10)$$

Both the coefficient  $b(z_o)$ , representing the flux of outgoing particles, and the energy factor  $N$ , corresponding to the potential of interest, are complex and are given explicitly in terms of the quantities present in Eq. (2) [67,68].

This derivation of the CESE does not involve the  $S$  matrix, as does the well-known Siegert treatment of resonant scattering [69], and reveals without restrictions as to the type of potential and of excitation process, the form of the complex—and lacking a Hilbert space norm [see Eq. (10)]—resonance eigenfunction,  $\psi(r; z_o)$ , of the CESE. This form consists of two parts, of which one,  $\psi_o$ , is square integrable and contains all the function space components contributing to the initial localization of the nonstationary state.

### B. Norm issue and complex scaling

The reliable solution of Eq. (9) presupposes the possibility of dealing effectively with all the difficulties of electronic structure, electron correlation, and open channel mixing, in addition to its non-Hilbert space character which is due to the fact that the resonance eigenfunction is unnormalizable. The last problem, known in nuclear physics since the *ad hoc* introduction of complex energies by Gamow, reduced for many decades the interest in tackling the problem of solving directly for the complex energy (pole of the resolvent on the second Riemann sheet), representing a resonance state even of a small system. For example, Kemble [70], in his 1937 book on quantum mechanics, discusses this issue in terms of the possibility of defining a new norm by introducing the attenuating factor  $e^{-ar^n}$ . This idea, and further analysis using short-range potentials, was much later examined by Zel'dovich [71] and Berggren [72].

In fact, a simple solution to the norm problem was proposed in 1961 by Dykhne and Chaplik [73] by extending integration into the upper half of complex coordinate plane, i.e., by changing  $r$  into  $re^{i\theta}$ . They showed that for the simple

model used by Zel'dovich, the same norm is obtained. They concluded that “*in spite of the fact that the wave functions vanish at infinity, the energy values are complex because of the non-Hermitian character of the Hamiltonian in  $\tilde{V}$* ” (the volume of integration). About a decade later, the same result was obtained in a mathematical language which analyzed the spectral properties of the rotated Coulomb Hamiltonian  $H(\theta) \equiv e^{-2i\theta}T + e^{-i\theta}V$  in the Hilbert space of  $\mathcal{L}^2$  functions [74–76]. It was shown that the complex eigenvalues of  $H(\theta)$  correspond to the second sheet poles of the resolvent, i.e., to resonance states. The computational implementation of the mathematical results was pioneered by Doolen and co-workers [53–55], whose findings showed that, in practice, the identification of the resonance eigenvalue in the midst of a plethora of irrelevant complex energies can be done by focusing on the kinks of stability appearing in the  $\theta$ -trajectories.

### C. Form of the trial resonance wave function for arbitrary atomic states and optimization of function spaces

It was recognized in the mid 1970s that the diagonalization of  $H(\theta)$  in a single basis set, a characteristic feature of the CCR calculations on two-electron resonance states which started at that time, is not practical for the calculation of more difficult cases or of polyelectronic states. [Discussions on resonance state calculations with different basis sets in conjunction with the  $H(\theta)$  Hamiltonian were initiated by Doolen and co-workers [53–55] and Bain *et al.* [77].] This limitation is analogous (but more severe) to the one present with the brute-force diagonalization of the real  $H$  for the calculation of discrete states. Furthermore, such an approach does not allow for a calculation of partial widths, although, on the positive side, it allows for a calculation of triply excited states where not only one- but also two-electron channels are open [64].

The bypass of this bottleneck is achieved by making the connection of the formalism of decaying states (Sec. IV A) with the requirement of regularizing the resonance eigenfunction. No transformation of the Hamiltonian coordinates is necessary. This has been discussed in a series of papers where emphasis was given to the possibility of obtaining efficiently accurate solutions to Eq. (9) for many-electron atomic and molecular nonstationary states, without or with the presence of a strong dc or ac electric or magnetic fields (see, Refs. [8,9,12,61,68], and references therein). The relations and equations which have gauged the strategy for dealing computationally with Eq. (9), as do the calculations of this work, were produced already in 1977–1980 [78,4,67] in forms expressing the notion of a two-part decaying state, where each part is represented by separately optimized function spaces, and where the asymptotic part containing the information about the energy shift and width is only an addendum of symmetry adapted complex functions.

For example, although the full implementation of the theory was delayed considerably due to the lack of computer power at the time, the first such calculations on the He  $2s2p\ ^1P^o$  resonance gave good results with a small expansion. The localized part was a numerical Hartree-Fock func-

tion together with correlation vectors such as  $2pd$ ,  $p'd'$ ,  $s'p''$ , etc., and the asymptotic part had Gamow orbitals  $g_j$  of the form

$$r^n \exp\left\{-k_j \exp\left[i\left(\theta - \alpha_j + \frac{3\pi}{2}\right)\right]\right\},$$

where  $k_j$  and  $\alpha_j$  were optimized subject to the virial theorem constraint. It was argued that on resonance, the general form of the expansion should be [4] (see section 7)

$$\psi = a(\theta)\psi_o + \sum_n b_n(\theta)u_n, \quad |a|^2 + \sum_n |b_n|^2 = 1 \quad (11)$$

with  $u_n$  being complex functions. In subsequent work, having already observed that most matrix elements in the non-Hermitian matrix remain the same when all coordinates are rotated, and with the availability of large computer memory and speed, it was found convenient to have the square integrable  $g_i$  for each channel  $i$ , expanded in terms of Slater or Gaussian orbitals. Thus the substitution of  $g_i$  by  $\mathcal{L}^2$  basis functions is

$$g^i(\rho) \rightarrow \sum_k C_k(\theta)\phi_k^i(r), \quad (12)$$

where, in practice, the construction of the non-Hermitian matrix is done by keeping all coordinates of the Hamiltonian operator and of the bound functions real, except for those of  $\phi_k^i$  for which  $r \rightarrow \rho^* = r e^{-i\theta}$ .

Optimization is carried out with respect to variations of  $\theta$ , of expansion size and of other nonlinear parameters in  $\phi_k^i$  (see Sec. V) searching for the stable root closest to  $E_o$  and with

$$|\langle \psi | \psi_o \rangle| = \max. \quad (13)$$

When more than one resonance state is searched for simultaneously, as in the present work, the construction and diagonalization of the complex matrix accounts for all direct and indirect interactions.

### V. THEORY: FEATURES OF THE H<sup>-</sup> RESONANCE SPECTRUM AS THEY RELATE TO THE PRESENT CALCULATIONS

According to the present decaying state viewpoint, the appearance of a resonance state in the continuous spectrum is the result of temporary wave-function localization caused by an effective multielectron potential particular to the state of interest. The localized state  $\psi_o$ , not being an eigenstate of the full Hamiltonian, is nonstationary and decays into the adjacent continuum with a rate whose magnitude depends primarily on the overlap of bound and scattering components near the nucleus [59].

A crucial element in the calculation of a resonance state, especially of the very difficult cases of the series of H<sup>-</sup> resonances treated here, is an efficient and at the same time numerically accurate determination of, first, a zero-order approximation of  $\psi_o$ , and, second, of the additional function

space which contributes to its localization. This zero-order approximation is usually multiconfigurational, especially for electrons in the same shell. In the case of H<sup>-</sup>, an understanding of the nature of configurations which are expected to mix when the effective multielectron potential providing the conditions for localization is created, can be obtained from existing results on two categories of wave functions for doubly excited states. In a full calculation, as in the present work, the basis set must contain the fine details of the functions of both categories since the exact  $\psi_o^k$  are superpositions of these.

The first category denoted here by  $\phi_n^o(I)$ , consists of combinations of intrashell configurations from the same hydrogen shell,  $n$ ,

$$\phi_n^o(I) = \sum_{l,l'} C_n^{l,l'} |(nl)(nl')\rangle, \quad (14)$$

where  $l, l'$  are dictated by the total symmetry of the state.

*Ab initio* results on the  $\phi_n^o(I)$  and their properties have been obtained for  $n$  up to 15 in a series of publications since 1986 (see Refs. [10,60,62], and references therein), for H<sup>-</sup> as well as for other small atoms and ANI's. Localization in zero order is obtained efficiently by calculating the radials self-consistently, with numerical as well as analytic techniques. Among other things, it was shown [60] via explicit computation of expectation values and conditional probability plots that the state of the lowest energy at each manifold has special geometrical properties, and constitutes a step in a ladder of resonances leading to a classically determined geometry at  $E=0$ , where the electrons are free. Additional results in Refs. [10,60,62] are also relevant to the understanding of the H<sup>-</sup> resonance spectrum and to the present calculations.

(1) The use of hydrogenic rather than self-consistent radials in  $\phi_n^o(I)$  gives poor results for the properties of these states. It follows that if fixed basis sets are used in the overall calculation of  $\psi_o^k$ , as in the present case, the space of single excitations corresponding to each  $\phi_n^o(I)$  must be represented extensively.

(2) As the energy excitation increases, double substitutions from  $\phi_n^o(I)$  influence more the wave-function characteristics than the total energy. It follows that in the calculation of a property sensitive to electron correlation such as the width, the function space for double excitations in H<sup>-</sup> resonance states must be very accurate. The recognition of the influence of double substitutions follows from the systematic examination of the degree of validity of the Herrick-Sinanoğlu [79] classification scheme of  $(K, T)$  quantum numbers, where the model space did not include pair excitations. It was found [62] that this classification deteriorates as  $n$  increases, even for the lowest-energy state of each intrashell manifold. By including pair correlations in the correlated wave functions, it was shown that a new scheme  $(F, T)$  provides a consistently better description of such states as well as of the others belonging to the same manifold. The quantum number  $F$  is defined as  $F = N - 1 - K$ , where  $N$  and  $K$  are no longer good numbers [62]. We note

that these conclusions were drawn after actual projection of correlated wave functions onto the  $(K, T)$  and  $(F, T)$  basis functions.

(3) Within the small uncertainty of the remaining energy shift due to the interaction with the function space representing the open channels, the energy spectrum of the lowest-energy intrashell resonances is given by a simple, yet generally applicable and computable, relation (see Ref. [60], and references therein)

$$-E_n = A \frac{n(n-1)}{r_n^2} \quad (15)$$

$$\approx \frac{A'}{n^2} \quad \text{for large } n, \quad (16)$$

where the radius  $r_n$  is obtained *ab initio* from the computed wave functions, and  $A$  is a constant characteristic of the symmetry of the ladder states. Equation (16) follows from Eq. (15) because it is found computationally that  $r_n \sim n^2$ . The dependence of  $E_n$  and especially of  $r_n$  on  $n^2$  constitutes a distinguishing feature for wave functions  $\phi_n^o(I)$  *vis a vis* those which are dominated by zero-order functions of the second category,  $\phi_n^o(II)$ , whose average  $r$  is defined essentially by the outer orbital in a range reaching thousands of a.u. for each threshold. In practical terms, this means that the two-electron basis sets which are used for the calculation of  $\psi_o^k$ , (mixtures of functions of both categories) must be large and flexible enough to represent both compact (relatively speaking) wave functions in the regions  $r \sim n^2$ , something like the ‘‘valence’’ states of neutral atoms, and diffuse wave functions associated with the ‘‘dipole resonances’’ discussed below.

The second category of  $H^-$  wave functions contains as zero-order wave functions for a particular symmetry the superposition of intershell configurations,

$$\phi_n^o(II) = \sum_{n', l, l'} C_n^{n', l, l'} |(nl)(n'l')\rangle, \quad (17)$$

where  $n' > n$ , and  $l, l'$  are dictated by the total symmetry of the state. It is immediately evident that now, as the difference between the values  $(nl)$  and  $(n'l')$  increases, the outer electron orbital becomes very diffuse, with exchange and correlation tending to zero. The question then is the following: Should one expect zero-order wave functions like  $\phi_n^o(II)$  to produce effective potentials of localization? Indeed, the answer is positive, and is given by the penetrating analysis by Gailitis and Damburg [13]. These authors made reasonable assumptions for the description of  $e^-$ -H scattering in the vicinity of each hydrogen threshold, and put forth an exactly solvable one-electron coupled-channel model of resonance creation in  $H^-$ . In this model, where only the large  $r$  part of the outer electron is considered, where exchange forces are neglected and where only the dipole term of the full Coulomb interaction is kept, localization is due to an attractive, one-electron effective potential, of the form  $1/r^2$ , characteristic of each degenerate threshold of hydrogen. This

potential is capable of supporting an infinity of bound states below each threshold which fall into one or more regular series. For each symmetry and threshold  $n$ , the energy spacings  $\epsilon_\kappa \equiv E(n) - E_\kappa(H^-)$  and the widths  $\Gamma_\kappa$  of each series are related by a fixed ratio

$$\frac{\epsilon_\kappa}{\epsilon_{\kappa+1}} = \frac{\Gamma_\kappa}{\Gamma_{\kappa+1}} = e^{(2\pi/lm\lambda)} = R, \quad \kappa = 2, 3, 4, \dots, \quad (18)$$

where  $\lambda$  is obtained from the theory of the model [13,17]. Furthermore, the extent of the *dipole resonance* wave functions also grows exponentially for successive states, with a long-range tail described by Hankel functions of the first kind [13–15]. It is then clear that the configurations in  $\phi_n^o(II)$  must involve an inner, compact orbital, and a numerically accurate very diffuse outer orbital.

Formulas (15) and (16) and other properties of  $H^-$  resonances whose zero-order wave functions are the  $\phi_n^o(I)$ , have been obtained via *ab initio* calculations including self-consistent radial relaxation and electron correlation (see Refs. [10,60], and references therein). On the other hand, the degree of satisfaction of the predicted regularity of the  $H^-$  resonance spectra below each threshold [Eq. (18)] has remained without quantitative verification or falsification, although some related discussion exists [13,34,45]. For this to be done reliably, a complete resolution of  $H^-$  resonance spectra of different symmetries up to a reasonable level of excitation, say up to the  $n=4$  or 5 thresholds should exist. Such a resolution implies the computation to high numerical accuracy, and to all orders in the interaction, of the direct and indirect mixing of correlated  $\psi_o^k$ , and of the continua into which they are embedded. The correlated  $\psi_o^k$  are superpositions of zero-order functions  $\phi_n^o(I)$  and  $\phi_n^o(II)$  and of configurations representing virtual one- and two-electron excitations into the function space of the closed channels.

The overall mixing produces resonance eigenfunctions with energies  $E_\kappa$  and widths  $\Gamma_\kappa$ , accumulating to a particular threshold, as well as the occasional appearance of a *shape resonance* just above this threshold. As regards the former, they correspond to the *dipole resonances* and offer the possibility of direct numerical comparison with Eq. (18) and, consequently, of the classification of the  $H^-$  spectra for each symmetry and threshold into perturbed and unperturbed spectra. As regards the latter, i.e., the resonances just above threshold, their wave functions are relatively compact, due to the dominant presence of intrashell functions  $\phi_n^o(I)$ . As energy increases, the probability of the appearance of shape resonances of different symmetries increases, since hydrogenic degeneracy is broadened, leading to larger numbers of  $\phi_n^o(I)$  and of different series of dipole resonances.

In closing this section, we point out that, as the title implies, what we discussed above regards the very accurate solution of the CESE and, consequently, the *ab initio* resolution of the  $H^-$  spectrum and the determination of the characteristics of the eigenfunctions (Sec. VI). In so doing, we adopted the Gailitis-Damburg approximation as the zero-order model not only to test the validity of its formal predictions but, especially, to utilize it for the purpose of classifi-

TABLE VI. The orbital basis set used in the present computation of  ${}^1P^o$ ,  ${}^1D^o$ , and  ${}^1F^o$  resonances. The number of localized radial STO's,  $N_{loc}$ , and the number of complex rotated radial STO's,  $N_{rot}$ , for each orbital symmetry  $l$  are given. The STO's are chosen systematically for groups of states so as to have their average  $r$  fall in a more or less regular way inside the range defined by  $\langle r \rangle_{min}$  and  $\langle r \rangle_{max}$ .

	$s$		$p$		$d$		$f$		$g$		$h$		$i$		$k$		$\langle r \rangle_{min}$	$\langle r \rangle_{max}$
	$N_{loc}$	$N_{rot}$	$N_{loc}$	$N_{loc}$														
${}^1P^o$	33	35	33	34	33	33	31	32	29		27		25				1.2	6600
${}^1D^o$			31	34	31	33	31	32	29		27		25				2.0	4300
${}^1F^o$	30	33	30	32	30	31	30	30	28	29	26	28	24	22			1.6	4500

cation of the computed complex eigenvalues and corresponding states into groups. (In Sec. VI we will see that in certain cases electron correlation causes the appearances of *loner* states, of overlapping resonances, and series perturbations, thereby destroying the regularities predicted by the model.) As regards previous attempts to classify doubly excited states of  $H^-$ , we already mentioned the Herrick-Sinanoglu ( $K, T$ ) scheme [79] and the more recent ( $F, T$ ) scheme [62]. Other work, based on approximate calculations of low-lying states below each threshold, or on models or on formal analysis leading to approximate quantum numbers can be found in Refs. [80–84].

#### Relativistic shape resonances?

The  $1/r^2$ -like effective potential and the model prediction of an infinity of “dipole resonances” result from the property of nonrelativistic hydrogenic degeneracy for  $n = 2, 3, 4, \dots$ . However, Gailitis and Damburg pointed out that in reality, the resonance series is truncated by the fine structure of the hydrogen thresholds. The question then is how many resonances of each symmetry actually exist in the neighborhood of each threshold. In response, Gailitis [13] employed a simple formula for the maximum number of resonances of each symmetry below the  $n = 3$  threshold. The same formula was later used by Pathak *et al.* [34], who prepared a related table. For example, for the  ${}^1P^o$  symmetry below the  $n = 2$  threshold, the prediction of Ref. [34] is that the number is 2. A more flexible treatment was done by Rotenberg and Cordes [16], who numerically solved the appropriate coupled-channel equations with explicit inclusion of threshold splittings.

Since the same theme was tackled again very recently for states below the  $n = 2$  threshold [43,44,85], this time the emphasis being on high numerical accuracy and explicit consideration of relativistic wave-function mixing, we would like

to make a related comment. The calculations of Refs. [43,85,44] were based either on the CCR method with numerical basis sets [43], or on coupled-channel scattering with model potentials [85,44], the latter aiming, as in Ref. [16], at determining the number of resonances for finite values of the splitting of the  $n = 2$  state. Both calculations were used to make specific predictions of the number of observable resonances. For example, consider the  ${}^1P^o$  symmetry. The conclusion of Ref. [43] is that there are only three  ${}^1P^o$  resonances. A fourth root of the CCR Hamiltonian matrix was discarded [43], as not representing a resonance state since its energy was found to be above the  $H\ 2p_{1/2}$  threshold. Thus in their Table II they reported the existence of only three  ${}^1P^o$  resonances, while a possible fourth resonance, for which a complex eigenvalue was obtained, is characterized as “non-existent.” The same conclusions are published in Ref. [44]: The introduction of relativistic corrections into relevant interaction matrices and to the  $n = 2$  threshold energy led to the result and conclusion that only “a third state is actually bound by about  $1.4 \times 10^{-6}$  Ry” [44]. (The same conclusion was reached about the  ${}^1S$  symmetry for which “all higher than four states are shifted above the  $p_{1/2}$  threshold and therefore disappear out of the series” [85]).

We would like to argue that the existence or not of resonances in  $H^-$ , or in any other spectrum of negative ions, need not depend exclusively and uniquely on whether the position of the predicted resonance lies below or above the corresponding threshold. In other words, a *resonance state may exist above its potential barrier or above its threshold*, in the nonrelativistic or in the relativistic (Dirac-Breit) spectrum. For example, the  ${}^1P^o$  resonance spectrum of  $H^-$  gives rise to the previously mentioned *shape* resonance just above the nonrelativistic  $n = 2$  threshold. Its existence implies that the residual Coulomb interactions, (or even relativistic ones), coupling the localized component to the open channels  $1s\epsilon p$ ,  $2s\epsilon p$ ,  $2p\epsilon s$ , and  $2p\epsilon d$ , are not sufficient to make this

TABLE VII. The basis set expansion for the CESE computation of  ${}^1P^o$ ,  ${}^1D^o$ , and  ${}^1F^o$  resonances. For a given total symmetry, the number of radial terms within the angular contribution  $ll'$  is given.

	$sp$	$pd$	$df$	$fg$	$gh$	$hi$	$sf$	$pg$	$dh$	$fi$	$gk$	Total
${}^1P^o$	998	822	675	576	511	435						4017
${}^1D^o$		869	768	689	601	519						3446
${}^1F^o$		701	606	534	456		756	621	520	468	395	5057

TABLE VIII.  $^1P^o$  shape resonance above the  $n=2$  H threshold. The real  $E$  and imaginary  $-\frac{1}{2}\Gamma$  parts of the complex energy, the energy position with respect to the  $n=2$  H threshold ( $-0.125$  a.u.)  $\delta E$ , and with respect to the  $H^-$  ground state  $\Delta E$  and the width  $\Gamma$ , are given. Our results are compared with the experimental [89,90,29] and theoretical ones obtained from the CCR [91,88,86],  $\mathcal{L}^2$  Feshbach [41], close-coupling [49], and  $R$ -matrix [34,36] methods.

Reference	$-E$ (a.u.)	$\frac{1}{2}\Gamma$ ( $10^{-4}$ a.u.)	$\delta E$ ( $10^{-5}$ a.u.)	$\Delta E$ (eV)	$\Gamma$ (meV)
present	0.124387	3.55	61.3	10.9697	19.3
[91]	0.124351	2.60	64.9	10.9707	14.1
[88]	0.12437		63.0	10.9702	18.5
[86]	0.12436	3.45	64.0	10.9705	18.8
[41]	0.12424		76.0	10.9737	22.6
[49]	0.124395	3.68	60.5	10.9695	20.0
[34]	0.124328	5.8	67.2	10.9713	32
[36]	0.124242	3.425	75.8	10.9737	18.6
Experiment					
[89]				10.971	21.2(11)
[90]				10.974(3)	20(1)
[90]				10.970(3)	30(1)
[29]				10.971(3) <sup>a</sup>	22(3)

<sup>a</sup>The result of Williams [29] is 10.217(3) eV above the  $1s$  H ground level; this result has been shifted to the  $1s^2 H^-$  position by the electron affinity 0.7544 eV.

spectral concentration disappear. Similarly, we expect that, if a series of nonrelativistically determined resonances for the lightest of atoms crosses a relativistic threshold, a resonance whose position is now above this new threshold will remain in existence, in spite of a possibly very weak binding, if the relativistic corrections cannot destroy its localization. Therefore, in order to prove the disappearance of such a resonance in a light atom, one would have to apply a rigorous theory of resonances with the Dirac-Breit one- and two-electron operators.

Our calculations (Secs. V and VI) produced a well-defined fourth complex eigenvalue above the  $2p_{1/2}$  threshold and below the  $2s_{1/2}$  one. Relativistic corrections will certainly affect slightly its energy and width. However, it is a moot point whether such weak interactions will wipe it out. It is also possible that they will simply transform it into a *relativistic shape resonance*.

## VI. CALCULATION AND RESULTS FOR THE $H^-$ $^1P^o$ , $^1D^o$ , AND $^1F^o$ RESONANCES

According to the contents of Secs. IV and V, the trial wave functions used in this work have two parts: a localized part, which is composed of functions of real coordinates accounting in a judicious way for the details, at large as well as at small  $r$ , of electronic structure and of electron correlation contributing to the stability of the state; and an asymptotic part, which is composed of two-electron configurations, where one set of basis representing the outgoing electron, is a function of  $re^{-i\theta}$  and, therefore, complex.

The hydrogen states associated with the open channels were represented by real Slater-type orbitals (STO's) with the exponents chosen to be equal to  $1/n$  so that, when combined, they can form the exact hydrogen functions. The real STO's which describe the localized part of the wave function, as well as those complex STO's (Gamow orbitals) that

TABLE IX. Results of the present CESE (complex eigenvalue Schrödinger equation) calculations for  $H^-$  resonances of  $^1P^o$  symmetry below the  $n=2$  threshold.  $E$ : total energy in a.u. (for  $H^-$ , 1 a.u. =  $27.211396 \times [M/(M+1)] = 27.19658$  eV).  $\Gamma$ : total width.  $\epsilon_m \equiv E_{th} - E_m$ : the energy distance from threshold.  $R_\epsilon \equiv \epsilon_{m-1}/\epsilon_m$ , and  $R_\Gamma \equiv \Gamma_{m-1}/\Gamma_m$ .

State	$-E$ (a.u.)	$\epsilon$ ( $10^{-9}$ a.u.)	$\Gamma/2$ ( $10^{-10}$ a.u.)	$R_\epsilon$	$R_\Gamma$
1	0.126 049 837	104 983 7.0	6809.0		
2	0.125 035 050 3	350 50.30	364.0	29.952	18.706
3	0.125 001 193 44	1193.44	13.2	29.369	27.576
4	0.125 000 040 8	40.80	0.1	29.251 <sup>a</sup>	
The value of the ratio given by the GD model is [17]				29.334	

<sup>a</sup>Because of the extreme diffuseness of this state function and of the corresponding small number for  $\Gamma$ , the value for  $R_\Gamma$  did not have the same level of accuracy, and therefore it is excluded from the list.

TABLE X. As in Table IX, for  $^1P^o H^-$  resonances below the  $n=3$  threshold. Two series are established, labeled *A* and *B*. Note the existence of overlapping resonances: *A3* and *B4*.

State	$-E$ (a.u.)	$\epsilon$ ( $10^{-8}$ a.u.)	$\frac{\Gamma}{2}$ ( $10^{-8}$ a.u.)	<i>A</i>		<i>B</i>	
				$R_\epsilon$	$R_\Gamma$	$R_\epsilon$	$R_\Gamma$
1 <i>A1</i>	0.062 716 92	716136	59503				
2 <i>B1</i>	0.058 571 809 6	301 625.40	449.37				
3 <i>B2</i>	0.056 116 399	560 84.3	112.89			5.378	3.981
4 <i>A2</i>	0.055 906 26	35070	3547.4	20.420	16.774		
5 <i>B3</i>	0.055 663 055 9	107 50.03	19.774			5.217	5.709
6 <i>A3</i>	0.055 576 361 2	2080.56	209.27	16.856	16.951		
7 <i>B4</i>	0.055 576 309 9	2075.43	10.015			5.180	1.974
8 <i>B5</i>	0.055 559 575 918	402.0362	0.7586			5.162	13.202
9 <i>A4</i>	0.055 556 795 29	123.973	12.849	16.782	16.287		
10 <i>B6</i>	0.055 556 333 474	77.7918	0.1451			5.168	5.228
11 <i>B7</i>	0.055 555 706 32	15.076	0.0294			5.160	4.935
12 <i>A5</i>	0.055 555 629 51	7.395	0.7640	16.763	16.818		
13 <i>B8</i>	0.055 555 583	2.7	0.55			5.493 <sup>a</sup>	
The values of the ratio given by the GD model are [17]				16.752		5.164	

<sup>a</sup>See the footnote of Table IX.TABLE XI. As in Tables IX and X, for  $^1P^o H^-$  resonances below the  $n=4$  threshold. Note the appearance of the state *D*, which does not belong to any of the three series, (*A*, *B*, and *C*), which are predicted by the GD model. This resonance overlaps with the neighboring ones, *B4* and *A4*.

State	$-E$ (a.u.)	$\epsilon$ ( $10^{-6}$ a.u.)	$\frac{\Gamma}{2}$ ( $10^{-8}$ a.u.)	<i>A</i>		<i>B</i>		<i>C</i>	
				$R_\epsilon$	$R_\Gamma$	$R_\epsilon$	$R_\Gamma$	$R_\epsilon$	$R_\Gamma$
1 <i>A1</i>	0.037 179 4	5929.4	51716.4						
2 <i>B1</i>	0.034 293 97	3043.97	916.4						
3 <i>A2</i>	0.032 350 629	1100.629	12076	5.387	4.283				
4 <i>B2</i>	0.032 198 287	948.287	396.08			3.210	2.314		
5 <i>C1</i>	0.031 613 080	363.080	297.9						
6 <i>B3</i>	0.031 555 16	305.16	135.8			3.108	2.917		
7 <i>A3</i>	0.031 497 50	247.50	3275	4.447	3.687				
8 <i>B4</i>	0.031 349 759	99.759	43.59			3.059	3.115		
9 <i>D</i>	0.031 322 98	72.98	5693.3						
10 <i>A4</i>	0.031 304 250	54.250	584.7	4.562	5.601				
11 <i>B5</i>	0.031 282 674	32.674	14.3			3.053	3.048		
12 <i>C2</i>	0.031 264 583 1	14.5831	13.07					24.897	22.79
13 <i>A5</i>	0.031 262 748 0	12.7480	125.55	4.256	4.657				
14 <i>B6</i>	0.031 260 682	10.682	4.7			3.059	3.043		
15 <i>B7</i>	0.031 253 511 4	3.5114	1.62			3.042	2.901		
16 <i>A6</i>	0.031 252 931 64	2.931 64	28.94	4.348	4.338				
17 <i>B8</i>	0.031 251 151 9	1.1519	0.527			3.048	3.074		
18 <i>A7</i>	0.031 250 672 53	0.672 53	6.69	4.359	4.326				
19 <i>C3</i>	0.031 250 535 34	0.535 34	0.475					27.241	27.516
20 <i>B9</i>	0.031 250 376 5	0.3765	0.190			3.059	2.774		
21 <i>A8</i>	0.031 250 154 2	0.1542	1.55	4.361	4.316				
22 <i>B10</i>	0.031 250 120	0.120	0.17			3.138	<sup>a</sup>		
23 <i>C4</i>	0.031 250 015 9	0.0159	0.067					<sup>a</sup>	<sup>a</sup>
24 <i>A9</i>	0.031 250 017 2	0.0172	0.9	<sup>a</sup>	<sup>a</sup>				
The values of the ratio given by the GD model are [17]				4.360		3.047		27.299	

<sup>a</sup>See the footnote of Table IX.

TABLE XII. As in Tables IX–XI, for  ${}^1D^o H^-$  resonances below the  $n=3$  threshold.

State	$-E$ (a.u.)	$\epsilon$ ( $10^{-9}$ a.u.)	$\frac{\Gamma}{2}$ ( $10^{-9}$ a.u.)	$R_\epsilon$	$R_\Gamma$
1	0.059 430 923	3875367	124955		
2	0.055 599 778 7	44223.1	1338.4	87.632	93.361
3	0.055 556 101 835	546.28	16.517	80.953	81.032
The value of the ratio given by the GD model is [17]				80.552	

describe the outgoing electron, were chosen so that their average  $r$  values formed geometrical sequence covering the region from  $\langle r \rangle_{min}$  to  $\langle r \rangle_{max}$ . The values of  $\langle r \rangle_{min}$  and  $\langle r \rangle_{max}$  are given in Table VI together with the number of localized STO's,  $N_{loc}$ , and complex rotated STOs,  $N_{rot}$ , for each orbital symmetry  $l$ . The rotated orbitals were combined with the STOs representing the hydrogen target states to form the two-electron configurations describing the asymptotic part of the wave function. The real localized STO's are used to construct the localized configurations. Since in the resonance states which are to be represented in such a basis set, one electron is supposed to be, on average, close to the nucleus, whereas the other one is diffuse, the whole orbital basis set was used for the outer electron and only half of it (the low  $\langle r \rangle$  part) was used for the inner electron. The number of configurations obtained in this way is given in Table VII together with the specification of angular  $ll'$  terms. The non-Hermitian Hamiltonian matrices were built from such basis and diagonalized for twelve values of  $\theta$  in the range from 0.2 rad up to 0.75 rad. The  $\langle r \rangle_{min}$  parameter was also optimized within a range of a few atomic (the values of  $\langle r \rangle_{min}$  given in Table VI determine the lowest limit for this range) units, in order to obtain the best  $\theta$  stabilization of the complex roots corresponding to the sought after resonances.

Our final results for the resonance energies and widths are presented in Tables I–III for  ${}^1P^o$ , and in Tables IV and V for  ${}^1D^o$  and  ${}^1F^o$  resonances below the  $n=3$  and 4 thresholds,

respectively. The decimal figures which are given were found to be stable against variation of  $\theta$ . Our results are compared with the most accurate and extensive previous calculations. Apart from the fact that only very few states, the ones lower lying in the region below a given threshold, were identified by the previous computations, it is noteworthy that some sequences of lower-lying resonances were incomplete with some states missing because of their small widths; see e.g., Tables III and V. In Table VIII we give our result for the only *shape* resonance we obtained, the  ${}^1P^o$  state lying above the  $n=2$  H threshold. It compares very well with results of other authors. Especially, it is in an agreement with data of Callaway [49] and of Ho and Bhatia [86].

The aim of our computation was to provide a complete list of resonances including extremely narrow and close to the threshold ones so that one can analyze general properties of the resonance spectrum and of the wave functions. Tables IX–XV are devoted to the analysis of regularity and of perturbances of the  $H^-$  resonance spectra. Given the prediction of the dipole approximation [13], we classified resonances into series according to the ratio,  $R_\epsilon \equiv \epsilon_{m-1}/\epsilon_m$ , where  $\epsilon_m \equiv E_{th} - E_m$ , and according to the ratio of their widths,  $R_\Gamma \equiv \Gamma_{m-1}/\Gamma_m$ . The GD model predicts that the ratios  $R_\epsilon$  and  $R_\Gamma$  should be the same for a given series as defined by Eq. (18). The values of this ratio, obtained by Pathak, Burke, and Berrington [17] are also given in the tables. It is seen that, for the cases of single series below a given threshold or of the

TABLE XIII. As in Tables IX–XII, for  ${}^1D^o H^-$  resonances below the  $n=4$  threshold. Note the existence of overlapping resonances: B3 and A6.

State	$-E$ (a.u.)	$\epsilon$ ( $10^{-6}$ a.u.)	$\frac{\Gamma}{2}$ ( $10^{-6}$ a.u.)	A		B	
				$R_\epsilon$	$R_\Gamma$	$R_\epsilon$	$R_\Gamma$
1 A1	0.036 529 2	5279.2	614.3				
2 A2	0.032 092 99	842.99	125.101	6.262	4.910		
3 B1	0.031 715 491 33	465.491 33	3.710 47				
4 A3	0.031 416 853	166.853	27.307	5.052	4.581		
5 A4	0.031 283 566 7	33.5667	5.6119	4.971	4.866		
6 B2	0.031 276 885 46	26.885 46	0.246 94			17.314	15.026
7 A5	0.031 256 778 6	6.7786	1.138	4.952	4.931		
8 B3	0.031 251 442 01	1.442 01	0.013 119			18.644	18.823
9 A6	0.031 251 371 95	1.371 95	0.230 92	4.941	4.928		
10 A7	0.031 250 277 7	0.2777	0.046 89	4.940	4.925		
11 B4	0.031 250 074 08	0.074 08	0.001 05			19.466 <sup>a</sup>	
The values of the ratio given by the GD model are [17]				4.940		18.777	

<sup>a</sup>See the footnote of Table IX.

TABLE XIV. As in Tables IX–XIII, for  ${}^1F^o H^-$  resonances below the  $n=3$  threshold.

State	$-E$ (a.u.)	$\epsilon$ ( $10^{-10}$ a.u.)	$\Gamma/2(10^{-10}$ a.u.)	$R_\epsilon$	$R_\Gamma$
1	0.056 558 751 9	10 031 963	250 34		
2	0.055 657 711 62	1 021 560.6	2770.1	9.820	9.037
3	0.055 566 431 70	108 761.4	298.6	9.393	9.277
4	0.055 556 720 982	116 54.26	32.04	9.332	9.320
5	0.055 555 680 9	1253	3.4	9.298	9.424
The value of the ratio given by the GD model is [17]				9.323	

lowest starting series,  $R_\epsilon$  converges to the model value from above, whereas  $R_\Gamma$  does so from below. This should be interpreted as a reflection of the fact that the lower-lying members of the series are bound more strongly, i.e., their positions are lower and they are more stable against autoionization than predicted by the GD model. On the other hand, higher series in general are less regular or not at all. For example, the  $C$  series of  ${}^1P^o$  resonances below the  $n=4$  threshold (Table XI) is quite irregular. The values of  $R_\epsilon$  at the beginning of the series are smaller than those predicted by the model. This means that the lower-lying members of such series are pushed up via the interaction with the parallel series. In the case of the  $C1$  and  $C2$   ${}^1F^o$  states (Table XV) the values of  $R_\epsilon$  and  $R_\Gamma$  differ by eight orders of magnitude from the GD model value. Finally, let us note that among the  ${}^1P^o$  states below the  $n=4$  threshold (see Table XI) there appears a loner state  $D$ , which does not belong to any of the series predicted by the model.

The classification of resonances into series is also supported by the recognition of their electron correlation pat-

terns. We consider the wave-function characteristics, including the estimate for the size of states due to the outer electron,  $\langle r_{out} \rangle$ , computed as the average of the distance of the outer electron from the nucleus, and the angular term contributions to the resonance wave functions. The resonances belonging to a given series have common angular electron correlation pattern; that is, they have the same contributions of various angular terms to their wave functions. If one considers the size of states, it changes regularly along a series. The ratio  $R_{\langle r \rangle} = \langle r_{out} \rangle_{m+1} / \langle r_{out} \rangle_m$  converges along a given series to a quite well-determined value which is characteristic for the series. For example, let us consider the  ${}^1P^o$  resonances below the  $n=4$  threshold, for which we give the wave-function characteristics in Table XVI [92]. The GD model predicts three series of resonances converging to this threshold. We have identified them by our computation and assigned the labels  $A$ ,  $B$ , and  $C$ . The dominant contributions to the  $A$  series wave functions come from the  $pd$  angular terms with important admixture of  $df$  and  $sp$  partial waves. In the  $B$  series, the  $sp$  terms play the leading role with con-

TABLE XV. As in Tables IX–XIV, for  ${}^1F^o H^-$  resonances below the  $n=4$  threshold. Note the existence of overlapping resonances:  $C1$  and  $B3$ .

State	$-E$ (a.u.)	$\epsilon$ ( $10^{-6}$ a.u.)	$\frac{\Gamma}{2}$ ( $10^{-6}$ a.u.)	$A$		$B$		$C$	
				$R_\epsilon$	$R_\Gamma$	$R_\epsilon$	$R_\Gamma$	$R_\epsilon$	$R_\Gamma$
1 $A1$	0.035 114 23	3864.23	327.5						
2 $B1$	0.033 461 482	2211.482	10.21						
3 $B2$	0.031 848 56	598.56	3.789			3.695	2.695		
4 $A2$	0.031 704 02	454.02	39.73	8.511	8.243				
5 $C1$	0.031 435 7	185.7	194.0						
6 $B3$	0.031 418 432	168.432	1.026			3.554	3.693		
7 $A3$	0.031 317 286	67.286	7.235	6.748	5.491				
8 $B4$	0.031 297 999	47.999	0.2910			3.509	3.526		
9 $C2$	0.031 274 6	24.6	10.3					7.549	18.835
10 $B5$	0.031 263 763 6	13.7636	0.0937			3.487	3.106		
11 $A4$	0.031 260 405	10.405	1.212	6.467	5.969				
12 $B6$	0.031 253 944 7	3.9447	0.0245			3.489	3.824		
13 $A5$	0.031 251 587 7	1.5877	0.1830	6.554	6.623				
14 $B7$	0.031 251 130 86	1.130 86	0.006 88			3.488	3.561		
15 $B8$	0.031 250 323 9	0.3239	0.002 36			3.491	2.915		
16 $A6$	0.031 250 243 3	0.2433	0.027 81	6.526	6.580				
17 $B9$	0.031 250 024	0.024	0.011			a	a		
The values of the ratio given by the GD model are [17]				6.496		3.485		8.516[8]	

<sup>a</sup>See footnote of Table IX.

TABLE XVI. Wave-function characteristics for the  $^1P^o H^-$  resonances lying below the  $n=4$  threshold.  $\langle r_{out} \rangle$  is the estimate for the size of each state due to the outer electron, computed as the average of the distance of the outer electron from the center of mass (in a.u.).  $R_{\langle r \rangle}$  is the ratio of consecutive values of  $\langle r_{out} \rangle$ . The notation  $[x]$  means  $10^{-x}$ . The  $D$  state does not belong to any of the three series predicted by the GD model.

State	$\langle r_{out} \rangle$	$R_{\langle r \rangle}$	$sp$	$pd$	$df$	$fg$	$gh$	$hi$
1 A1	35.20		0.289	0.563	0.144	0.5[2]	0.7[5]	0.5[7]
3 A2	71.74	2.038	0.249	0.551	0.190	0.011	0.4[4]	0.6[7]
7 A3	151.4	2.110	0.215	0.542	0.226	0.017	0.2[4]	0.3[7]
10 A4	314.9	2.080	0.205	0.511	0.258	0.027	0.1[3]	0.1[6]
13 A5	666.3	2.116	0.196	0.521	0.257	0.025	0.1[4]	0.1[7]
16 A6	1397	2.097	0.198	0.520	0.257	0.025	0.3[5]	0.2[8]
18 A7	2920	2.090	0.195	0.520	0.260	0.025	0.6[6]	0.5[9]
21 A8	6095	2.087	0.195	0.519	0.261	0.026	0.1[6]	0.1[9]
24 A9	9679	1.588	0.235	0.508	0.240	0.017	0.6[7]	0.5[10]
2 B1	53.54		0.610	0.338	0.050	0.2[2]	0.5[5]	0.1[7]
4 B2	96.41	1.801	0.585	0.352	0.062	0.3[2]	0.4[5]	0.8[8]
6 B3	172.0	1.784	0.568	0.355	0.073	0.4[2]	0.1[4]	0.1[7]
8 B4	308.3	1.792	0.550	0.369	0.077	0.4[2]	0.6[6]	0.9[9]
11 B5	543.8	1.764	0.543	0.372	0.081	0.4[2]	0.2[6]	0.3[9]
14 B6	953.3	1.753	0.539	0.372	0.084	0.5[2]	0.3[6]	0.3[9]
15 B7	1675	1.757	0.529	0.377	0.089	0.6[2]	0.2[7]	0.3[10]
17 B8	2928	1.749	0.529	0.377	0.088	0.6[2]	0.8[8]	0.1[10]
20 B9	5109	1.745	0.528	0.376	0.090	0.6[2]	0.7[8]	0.8[11]
22 B10	8549	1.673	0.516	0.384	0.094	0.6[2]	0.1[8]	0.2[11]
5 C1	77.59		0.271	0.172	0.490	0.067	0.4[3]	0.5[6]
12 C2	319.0	4.111	0.295	0.116	0.495	0.095	0.3[4]	0.3[7]
19 C3	1578	5.948	0.302	0.102	0.493	0.103	0.1[5]	0.1[8]
23 C4	6858	4.346	0.315	0.092	0.493	0.101	0.6[7]	0.6[10]
9 D	55.32		0.304	0.059	0.489	0.146	0.2[2]	0.2[5]

tributions from the  $pd$  configurations. In the  $C$  resonances the angular correlation is richer. Here the  $df$  terms constitute the main part of the wave function together with a large addition of  $sp$  terms. The  $pd$  and  $fg$  contributions, though three times smaller than the  $sp$  contribution, are not negligible. Finally, the state  $D$  corresponds to a wave function which bears some resemblance to the  $C$  case. However, the sharing of  $pd$  and  $fg$  contributions is different. Moreover, the radial distribution of the electron density, represented by the  $\langle r_{out} \rangle$  values, does not fit the pattern for the  $C$  series, for which the  $R_{\langle r \rangle}$  is about 5, while the  $\langle r_{out} \rangle$  value for the  $D$  state is smaller than that of the  $C1$  state lying below  $D$ . Hence we have concluded that the  $D$  state is not a member of the series  $C$ .

One can see that in all the cases of single series these are regular and the characteristic ratios  $R_\epsilon$ ,  $R_\Gamma$ , and  $R_{\langle r \rangle}$  converge very well, in most cases monotonically. If there are two or more series of resonances of the same symmetry in a given region, they exhibit perturbations. The situation becomes extremely interesting when accidentally two resonances overlap, i.e., their energy difference is smaller than or

comparable to the width of at least one of such states. One can find such overlapping resonances in Tables X, XI, XIII, and XV. The overlapping  $A3$  and  $B4$   $^1P^o$  resonances lying below the  $n=3$  threshold (Table X) can also be recognized in the results of Venuti and Decleva [42]. However, there are two differences: First, in our case the narrower state,  $B4$ , lies above the broader one,  $A3$ , whereas the result of Ref. [42] is the opposite. Second, in our case the overlap is stronger because the energy difference is five times smaller than that predicted by Venuti and Decleva [42]. An interesting case is the  $^1P^o$  resonances below the  $n=4$  threshold, where resonance  $D$  overlaps with its two neighbors:  $B4$ , lying below, and  $A4$ , lying above. The appearance of the loner resonance  $D$ , which is not predicted by the dipole model, is a result of strong correlation and exchange effects not taken into account by this model.

## VII. SYNOPSIS

Given certain characteristics of the  $H^-$  resonance spectra, identified quantitatively from the Gailitis-Damburg model of dipole resonances, we defined demanding cutoff criteria and solved to very high accuracy, via the systematic and group-of-states-specific choice and optimization of real and complex functions, the matrix complex eigenvalue Schrödinger equation, for all states of  $^1P^o$ ,  $^1D^o$ , and  $^1F^o$  symmetry, up to the  $n=4$  threshold (see, Ref. [1] for results on  $^1S$  and  $^1D$  states up to the  $n=4$ , threshold and Ref. [2] for results on  $^1P$  states up to the  $n=5$  threshold). We suggest that at least a subset of the theoretically identified resonances should be observable in sophisticated experiments based on multistep excitation mechanisms and ultrasensitive detection techniques.

This *ab initio* approach to the problem defined herein, i.e., to the possibility of resolving completely the resonance spectrum of a multiparticle system with a reasonably large and physically relevant span of its continuous spectrum, has provided a wealth of new and significant information on each resonance individually as well as on the spectral features collectively. As regards the latter, it was shown that, by adopting the Gailitis-Damburg model as the zero-order model, the resonance spectra of  $H^-$  can be classified into two groups, just as it is possible to do with the spectra of neutral atoms and positive ions, where the zero order potential can be taken as having the Coulomb  $1/r$  form. The first group contains unperturbed series whose energies and widths satisfy the GD conditions of Eq. (18), and have similar angular correlation characteristics. The second group contain perturbed series and loner states, with the occasional existence of strongly overlapping resonances.

## ACKNOWLEDGMENTS

Support to one of us (M.B.) from the National Technical University of Athens is gratefully acknowledged. This work was supported by the Polish Committee for Scientific Research (Grant No. KBN 2 P03B 125 18).

- [1] M. Bylicki and C. A. Nicolaides, *Phys. Rev. A* **61**, 052509 (2000).
- [2] M. Bylicki and C. A. Nicolaides, *J. Phys. B* **32**, L317 (1999).
- [3] C. A. Nicolaides, *Phys. Rev. A* **6**, 2078 (1972).
- [4] C. A. Nicolaides and D. R. Beck, *Int. J. Quantum Chem.* **14**, 457 (1978).
- [5] Y. Komninos, G. Aspromallis, and C. A. Nicolaides, *Phys. Rev. A* **27**, 1865 (1983).
- [6] C. A. Nicolaides and Th. Mercouris, *Phys. Rev. A* **32**, 3247 (1985).
- [7] M. Chrysos, Y. Komninos, Th. Mercouris, and C. A. Nicolaides, *Phys. Rev. A* **42**, 2634 (1990).
- [8] Th. Mercouris and C. A. Nicolaides, *J. Phys. B* **24**, L557 (1991).
- [9] M. Bylicki and C. A. Nicolaides, *Phys. Rev. A* **48**, 3589 (1993); M. Bylicki, S. I. Themelis, and C. A. Nicolaides, *J. Phys. B* **27**, 2741 (1994).
- [10] S. I. Themelis and C. A. Nicolaides, *J. Phys. B* **28**, L379 (1995).
- [11] Th. Mercouris and C. A. Nicolaides, *J. Phys. B* **30**, 811 (1997).
- [12] C. A. Nicolaides, *Int. J. Quantum Chem.* **71**, 209 (1999); **60**, 119 (1996).
- [13] M. Gailitis and R. Damburg, *Proc. Phys. Soc. London* **82**, 192 (1963); M. Gailitis, *J. Phys. B* **13**, L479 (1980).
- [14] A. Temkin and J. F. Walker, *Phys. Rev. A* **140**, A1520 (1965).
- [15] J. C. Y. Chen and M. Rotenberg, *Phys. Rev.* **166**, 7 (1968).
- [16] M. Rotenberg and M. R. Cordes, *J. Phys. B* **5**, 2225 (1972).
- [17] A. Pathak, P. G. Burke, and K. A. Berrington, *J. Phys. B* **22**, 2759 (1989).
- [18] M. Gailitis and R. Damburg [13] pointed out that in fact the series of the dipole resonances terminate because of the lifting of the hydrogen degeneracy caused by the relativistic splitting. A related comment is given in our Sec. IV.
- [19] N. A. Piangos and C. A. Nicolaides, *J. Phys. B* **31**, L147 (1998).
- [20] M. Halka, H. C. Bryant, E. P. Mackerrow, W. Miller, A. H. Mohagheghi, C. Y. Tang, S. Cohen, J. B. Donahue, A. Hsu, C. R. Quick, J. Tice, and K. Rozsa, *Phys. Rev. A* **44**, 6127 (1991).
- [21] H. H. Andersen, P. Balling, P. Kristensen, U. V. Pedersen, S. A. Aseyev, V. V. Petrunin, and T. Andersen, *Phys. Rev. Lett.* **79**, 4770 (1997).
- [22] A. Stintz, X. M. Zhao, C. E. M. Strauss, W. B. Ingalls, G. A. Kyrala, D. J. Funk, and H. C. Bryant, *Phys. Rev. Lett.* **75**, 2924 (1995).
- [23] For easy reference, the relevant energy value, the infinite mass atomic unit, is 27.211396 eV. Using the reduced mass for hydrogen, 1 a.u.=27.19658 eV. The hydrogen threshold energies are  $E_{n=2} = -0.125$  a.u., i.e., 10.19872 eV above H 1s;  $E_{n=3} = -0.0555556$  a.u., i.e., 12.08737 eV above H 1s; and  $E_{n=4} = -0.03125$  a.u., i.e., 12.74840 eV above H 1s. The total (relativistic) energy of  $H^- 1s^2 1S$  is  $-0.5277317$  a.u.. The non-relativistic total energy of  $H^-$  is  $-0.5277510$  a.u. [G. W. Drake, *Nucl. Instrum. Methods Phys. Res. B* **31**, 7 (1988)].
- [24] J. W. McGowan, *Phys. Rev.* **156**, 165 (1967); J. W. McGowan, J. F. Williams, and E. K. Curley, *ibid.* **180**, 132 (1969).
- [25] G. J. Schulz, *Rev. Mod. Phys.* **45**, 378 (1973).
- [26] J. S. Risley, A. K. Edwards, and R. Geballe, *Phys. Rev. A* **9**, 1115 (1974).
- [27] J. F. Williams, in *Progress in Atomic Spectroscopy*, edited by W. Hanle and H. Kleinpoppen (Plenum Press, New York, 1979), p. 1031.
- [28] C. D. Warner, G. C. King, P. Hammond, and J. Slevin, *J. Phys. B* **19**, 3297 (1986); C. D. Warner, P. M. Rutter, and G. C. King, *ibid.* **23**, 93 (1990).
- [29] J. F. Williams, *J. Phys. B* **21**, 2107 (1988).
- [30] E. Träbert, P. H. Heckmann, J. Doerfert, and J. Granzow, *J. Phys. B* **25**, L353 (1992).
- [31] Y. Komninos and C. A. Nicolaides, *J. Phys. B* **30**, L237 (1997).
- [32] L. Sanche and P. D. Burrow, *Phys. Rev. Lett.* **29**, 1639 (1972).
- [33] S. J. Buckman and C. W. Clark, *Rev. Mod. Phys.* **66**, 539 (1994).
- [34] A. Pathak, A. E. Kingston, and K. A. Berrington, *J. Phys. B* **21**, 2939 (1988).
- [35] B. R. Odgers, M. P. Scott, and P. G. Burke, *J. Phys. B* **28**, 2973 (1995).
- [36] H. R. Sadeghpour, C. H. Greene, and M. Cavagnero, *Phys. Rev. A* **45**, 1587 (1992); H. R. Sadeghpour and C. H. Greene, *Phys. Rev. Lett.* **65**, 313 (1990).
- [37] Y. K. Ho, *Phys. Rev. A* **23**, 2137 (1981).
- [38] Y. K. Ho, *Chin. J. Phys. (Taipei)* **29**, 327 (1991).
- [39] T. F. O'Malley and S. Geltman, *Phys. Rev.* **137**, A1344 (1965).
- [40] G. J. Seiler, R. S. Oberoi, and J. Callaway, *Phys. Rev. A* **3**, 2006 (1971).
- [41] M. Cortés and F. Martín, *Phys. Rev. A* **48**, 1227 (1993).
- [42] M. Venuti and P. Decleva, *J. Phys. B* **30**, 4839 (1997).
- [43] E. Lindroth, A. Bùrgers, and N. Brandefelt, *Phys. Rev. A* **57**, R685 (1998).
- [44] T. Purr and H. Friedrich, *Phys. Rev. A* **57**, 4279 (1998).
- [45] T. T. Gien, *J. Phys. B* **31**, L1001 (1998).
- [46] As regards the region above the  $n=4$  threshold, which is out of interest of this work, a few  $^1P^o$  resonances have been predicted, e.g., between  $n=4$  and 7, by J. Z. Tang and I. Shimamura, *Phys. Rev. A* **51**, R1738 (1995). This paper pays attention to the Wannier states up to the  $n=7$  threshold. Such results were obtained much earlier by C. A. Nicolaides and Y. Komninos, [*ibid.* **35**, 999 (1987)] for the Wannier states up to the  $n=10$  threshold.
- [47] M. Chrysos, Y. Komninos, and C. A. Nicolaides, *J. Phys. B* **25**, 1977 (1992).
- [48] L. A. Morgan, M. R. C. McDowell, and J. Callaway, *J. Phys. B* **10**, 3297 (1977).
- [49] J. Callaway, *Phys. Rev. A* **26**, 199 (1982).
- [50] J. Callaway, *Phys. Rev. A* **37**, 3692 (1988).
- [51] L. Lipsky, R. Anania, and M. J. Connelly, *At. Data Nucl. Data Tables* **20**, 127 (1977).
- [52] The use of unoptimized bound hydrogenic functions in a single diagonalization without the contribution of the open channels cannot establish the correspondence of a root with a resonance state.
- [53] G. D. Doolen, J. Nuttall, and R. W. Stagat, *Phys. Rev. A* **10**, 1612 (1974).
- [54] G. D. Doolen, *J. Phys. B* **8**, 525 (1975).
- [55] G. D. Doolen, *Int. J. Quantum Chem.* **14**, 523 (1978).
- [56] Y. K. Ho and J. Callaway, *Phys. Rev. A* **34**, 130 (1986).
- [57] Y. K. Ho, *Phys. Lett. A* **189**, 374 (1994).
- [58] A. K. Bhatia and Y. K. Ho, *Phys. Rev. A* **50**, 4886 (1994).

- [59] C. A. Nicolaides, N. Makri, and Y. Komninos, *J. Phys. B* **20**, 4963 (1987).
- [60] Y. Komninos and C. A. Nicolaides, *Phys. Rev. A* **50**, 3782 (1994).
- [61] C. Haritos, Th. Mercouris, and C. A. Nicolaides, *J. Phys. B* **31**, L783 (1998).
- [62] Y. Komninos, S. I. Themelis, M. Chrysos, and C. A. Nicolaides, *Int. J. Quantum Chem., Symp.* **27**, 399 (1993).
- [63] M. Bylicki, *J. Phys. B* **30**, 189 (1997).
- [64] M. Bylicki and C. A. Nicolaides, *J. Phys. B* **31**, L685 (1998).
- [65] U. Fano, *Phys. Rev.* **124**, 1866 (1961).
- [66] H. Feshbach, *Ann. Phys. (N.Y.)* **19**, 287 (1962).
- [67] C. A. Nicolaides, Y. Komninos, and Th. Mercouris, *Int. J. Quantum Chem., Symp.* **15**, 355 (1981).
- [68] C. A. Nicolaides and S. I. Themelis, *Phys. Rev. A* **45**, 349 (1992); S. I. Themelis and C. A. Nicolaides, *ibid.* **59**, 2500 (1999).
- [69] A. F. J. Siegert, *Phys. Rev.* **56**, 750 (1939).
- [70] E. C. Kemble, *The Fundamental Principles of Quantum Mechanics* (McGraw-Hill, New York, 1937), Sec. 31f.
- [71] Ya. B. Zel'dovich, *Zh. Éksp. Teor. Fiz.* **39**, 776 (1960) [*Sov. Phys. JETP* **12**, 542 (1961)].
- [72] T. Berggren, *Nucl. Phys. A* **109**, 265 (1968).
- [73] A. M. Dykhne and A. V. Chaplik, *Zh. Éksp. Teor. Fiz.* **40**, 1427 (1961) [*Sov. Phys. JETP* **13**, 1002 (1961)].
- [74] J. Aguilar and J. M. Combes, *Commun. Math. Phys.* **22**, 269 (1972).
- [75] E. Balslev and J. M. Combes, *Commun. Math. Phys.* **22**, 280 (1972).
- [76] B. Simon, *Commun. Math. Phys.* **27**, 1 (1972).
- [77] R. A. Bain, J. N. Bardsley, B. R. Junker, and C. V. Sukumar, *J. Phys. B* **7**, 2189 (1974).
- [78] C. A. Nicolaides and D. R. Beck, *Phys. Lett.* **65A**, 11 (1978); C. A. Nicolaides, H. J. Gotsis, M. Chrysos, and Y. Komninos, *Chem. Phys. Lett.* **168**, 570 (1990).
- [79] D. R. Herrick and O. Sinanoğlu, *Phys. Rev. A* **11**, 97 (1975).
- [80] D. R. Herrick, *Phys. Rev. A* **12**, 413 (1975).
- [81] S. I. Nikitin and V. N. Ostrovsky, *J. Phys. B* **9**, 3141 (1976).
- [82] D. R. Herrick, M. E. Kellman, and R. D. Poliak, *Phys. Rev. A* **22**, 1517 (1980).
- [83] C. D. Lin, *Adv. At. Mol. Phys.* **22**, 77 (1986).
- [84] J. M. Rost and J. S. Briggs, *J. Phys. B* **24**, 4293 (1991).
- [85] T. Purr, H. Friedrich, and A. T. Stelbovics, *Phys. Rev. A* **57**, 308 (1998).
- [86] Y. K. Ho and A. K. Bhatia, *Phys. Rev. A* **48**, 3720 (1993).
- [87] Y. K. Ho, *Phys. Rev. A* **45**, 148 (1992).
- [88] E. Lindroth, *Phys. Rev. A* **52**, 2737 (1995).
- [89] H. C. Bryant, D. A. Clark, K. B. Butterfield, C. A. Frost, H. Sharifian, H. Tootoonchi, J. B. Donahue, P. A. M. Gram, M. E. Hamm, R. W. Hamm, J. C. Pratt, M. A. Yates, and W. W. Smith, *Phys. Rev. A* **27**, 2889 (1983).
- [90] M. Halka, H. C. Bryant, C. Johnstone, B. Marchini, W. Miller, A. H. Mohagheghi, C. Y. Tang, K. B. Butterfield, D. A. Clark, S. Cohen, J. B. Donahue, P. A. M. Gram, R. W. Hamm, A. Hsu, D. W. MacArthur, E. P. MacKerrow, C. R. Quick, J. Tiee, and K. Rózsa, *Phys. Rev. A* **46**, 6942 (1992).
- [91] J. J. Wendoloski and W. P. Reinhardt, *Phys. Rev. A* **17**, 195 (1978).
- [92] Tables containing the wave-function characteristics for all the states under consideration can be obtained from [ftp://ftp.phys.uni.torun.pl/pub/publications/ifiz/mirekb/H/\\_tab\\_I.ps](ftp://ftp.phys.uni.torun.pl/pub/publications/ifiz/mirekb/H/_tab_I.ps).